Check for updates

Fabrication of Insoluble Elastin by Enzyme-Free Cross-Linking

Tobias Hedtke, Mathias Mende, Heiko Steenbock, Jürgen Brinckmann, Matthias Menzel, Wolfgang Hoehenwarter, Markus Pietzsch, Thomas Groth, and Christian E. H. Schmelzer*

Elastin is an essential extracellular matrix protein that enables tissues and organs such as arteries, lungs, and skin, which undergo continuous deformation, to stretch and recoil. Here, an approach to fabricating artificial elastin with close-to-native molecular and mechanical characteristics is described. Recombinantly produced tropoelastin are polymerized through coacervation and allysine-mediated cross-linking induced by pyrroloquinoline quinone (PQQ). A technique that allows the recovery and repeated use of PQQ for protein cross-linking by covalent attachment to magnetic Sepharose beads is developed. The produced material closely resembles natural elastin in its molecular, biochemical, and mechanical properties, enabled by the occurrence of the cross-linking amino acids desmosine, isodesmosine, and merodesmosine. It possesses elevated resistance against tryptic proteolysis, and its Young's modulus ranging between 1 and 2 MPa is similar to that of natural elastin. The approach described herein enables the engineering of mechanically resilient, elastin-like materials for biomedical applications.

1. Introduction

Elastin is a major constituent of the elastic fibers in the extracellular matrix. It is a highly cross-linked and metabolically stable biopolymer that provides elasticity and resilience to tissues that are required to withstand repeated cycles of stretch and recoil. Elastin's presence is vital to the function of tissues such as those of arteries, lungs, tendons, cartilage, and skin. The multistep biosynthesis pathway of elastic fibers, termed elastogenesis, sets in during embryonic development and reaches its maximum near birth (see[1] for review). Postnatal elastogenesis in mammals is dramatically reduced and virtually absent in adults.[2,3] The resulting high biological half-life has been determined to be 74 years in humans.[4] The ≈60 kDa monomeric elastin precursor protein tropoelastin (TE) is expressed in elastogeneic cells (e.g., fibroblasts, chondrocytes, and vascular smooth muscle cells) and secreted to the extracellular space. The primary structure of TE resembles the exon structure of its gene and is characterized by an alternating pattern of hydrophobic sequences rich in alanine (Ala), valine (Val), glycine (Gly), proline (Pro), and hydrophilic lysine (Lys)-containing regions.[5] The exon equivalents are commonly referred to as domains. Lys-rich domains are involved in extensive cross-linking and can be divided into Lys-Ala (KA) domains, where adjacent pairwise Lys residues are surrounded by Ala-rich sequences (KAAK, KAAAK, and KxAAK), and Lys-Pro (KP) domains containing at least one Pro residue between the Lys pair (KPK, KxPK, and KPxK).[6] In the extracellular space, TE monomers assemble in a process termed coacervation.

T. Hedtke, M. Menzel, C. E. H. Schmelzer
Department of Biological and Macromolecular Materials
Fraunhofer Institute for Microstructure of Materials and Systems IMWS
06120 Halle (Saale), Germany
E-mail: schmelzer@pharmazie.uni-halle.de

T. Hedtke, M. Mende, M. Pietzsch, T. Groth, C. E. H. Schmelzer
Institute of Pharmacy, Faculty of Natural Sciences I
Martin Luther University Halle-Wittenberg, Halle (Saale)
06120 Halle (Saale), Germany

H. Steenbock, J. Brinckmann
Institute of Virology and Cell Biology
University of Lübeck
23562 Lübeck, Germany

J. Brinckmann
Department of Dermatology
University of Lübeck
23538 Lübeck, Germany

W. Hoehenwarter
Proteome Analytics Research Group
Leibniz Institute for Plant Biochemistry
06120 Halle (Saale), Germany

M. Pietzsch, C. E. H. Schmelzer
Institute of Applied Dermatopharmacy at the Martin Luther University
Halle-Wittenberg (IADP)
06120 Halle (Saale), Germany

T. Groth
Interdisciplinary Center of Materials Science
Martin Luther University Halle-Wittenberg
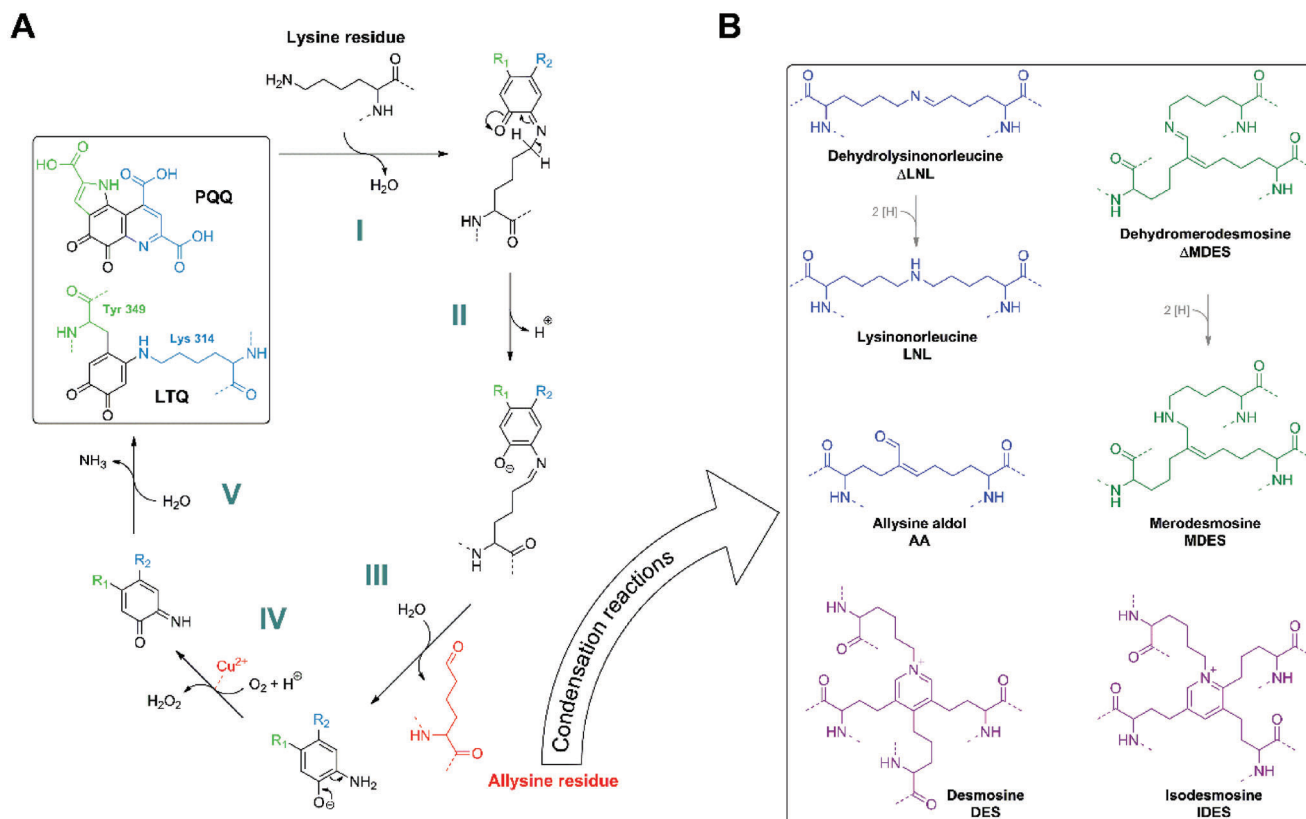06120 Halle (Saale), Germany

A

B

Figure 1. Mechanism of oxidative deamination and abundant cross-linking structures in elastin. A) The catalytic cycle of LTQ- and PQQ-mediated lysine modification basically consists of two phases: oxidative deamination (I-III) and *ortho*-quinone regeneration (IV, V). In this, the primary ϵ-amine of peptidyl lysine condenses with one of the quinonic carbonyl groups to form a quinone ketimine intermediate (I) that is subsequently converted to quinolaldimine by proton abstraction (II). From this intermediate allysine is released by hydrolysis (III) and LTQ/PQQ regeneration is initiated by Cu^{2+}-mediated oxidation of their aminophenol form (IV) to give quinoneimine. Reoxidation of Cu+ formed during the reaction is done by molecular oxygen present in the reaction mixtures. Finally, the *ortho*-quinone of LTQ/PQQ is regenerated by hydrolysis of the latter intermediate. Scheme adapted from.[14,15] B) Overview of the major cross-linking amino acids in elastin that are formed from condensation reactions. Bifunctional, trifunctional, and tetrafunctional cross-links are shown in blue, green, and purple, respectively.

Subsequently, the Cu^{2+}-dependent enzymes lysyl oxidase (LOX) and lysyl oxidase-like (LOXL) 1 and 2 then catalyze the oxidative deamination of the ϵ-amino group of Lys residues of KA and KP domains leading to the formation of the reactive allysine (Lya) residues (see **Figure 1**A).[7–10] Subsequent condensation reactions of Lys and Lya result in the covalent polymerization of TE by forming a heterogeneous cross-linking pattern.[11,12] Among the characteristic cross-linking, amino acids (Figure 1B) are the tetrafunctional pyridine-based amino acids desmosine (DES) and isodesmosine (IDES). Detailed information on the molecular structure is summarized in a recent review.[13]

In vertebrates such as chickens, humans, pigs, and cows, there is virtually no elastin turnover and elastic tissue is not regenerated properly upon injury. Hence, although it is an extremely durable protein, elastin undergoes progressive degradation throughout life as a consequence of aging processes and pathologic conditions. These processes cause changes in the microstructure of the elastic fiber network,[16] which in turn can lead to a reduction or even loss of function of tissues and organs.[17] Therefore, materials need to be developed that compensate for the loss of elasticity due to elastin degradation in different tissues like skin and vasculature. Due to demographic change, this

field of research is of particular importance since many age-related diseases result in elastin damage or are caused by progressive elastin degradation. For this purpose, key steps of elastogenesis are replicated in vitro, especially with respect to self-assembly and cross-linking. Various biomaterials based on TE-synthesized elastin peptides or hydrolyzed elastin with elastin-like properties have been made utilizing methods like electrospinning, lyophilization, gelation, or foaming.[18]

We have recently demonstrated the production of highly elastic biomaterials from human TE through in vitro cross-linking using recombinant human LOXL2.[10] While the material showed remarkable similarities to mature elastin, its usage is currently limited to the lab scale due to high production costs and low availability of LOXL2. In this study, we focus on the fabrication of artificial elastin by inducing LOX-like cross-linking of recombinant human TE in an enzyme-free approach using pyrroloquinoline quinone (PQQ, Figure 1A). PQQ is a redox cofactor and the prosthetic group of quinoproteins in bacteria (for review see[19]). According to current knowledge, there are no PQQ-dependent enzymes in mammals but nonetheless, trace amounts of PQQ were found in rat and human tissues. As it is not synthesized in mammals its origin is rather explained as being a ubiquitous
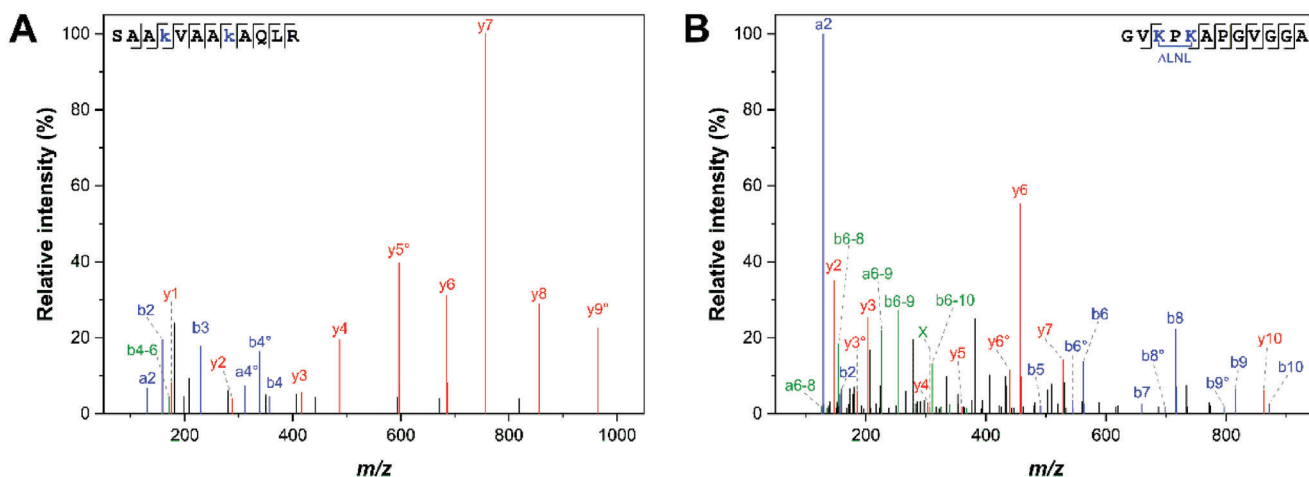
**ADVANCED
SCIENCE NEWS**

www.advancedsciencenews.com

**Macro-
molecular**
Bioscience

www.mbs-journal.de

Figure 2. Tandem mass spectra of modified peptides from cTE. A) Fragment ion mass spectrum of a cTE peptide released from domain 25. Both lysine residues of a cross-linking motif are transformed to allysine. The peptide sequence with the highlighted modified residues and the observed fragmentation pattern is given in the top left corner. B) This product ion mass spectrum results from an internally cross-linked cTE peptide, in which both former lysine residues of the cross-linking motif of domain 10 are interconnected by ΔLNL. The peptide sequence with the highlighted cross-link and the observed fragmentation pattern is given in the top right corner. a and b ions are colored blue, y ions are depicted in red and internal fragments with a or b ion structures are colored green. The neutral loss of water is indicated by °. The internal fragment labeled with "X" in (B) refers to the immonium ion of the cross-linking structure. The precursor peptide ions were detected with m/z 606.3397 (z = 2, $\Delta m = -1.8$ ppm) and m/z 509.7878 (z = 2, $\Delta m = -0.7$ ppm) at retention times of 39.22 min and 28.49 min for (A) and (B), respectively.

part of nutrition.[20] The presence of quinoenzymes is not limited to prokaryotes as several eukaryotic enzymes exist that depend on intrinsic quino-cofactors (for review see[21,22]). Among them, lysyl tyrosylquionone (LTQ, Figure 1A) is the cofactor of LOX(L) enzymes and emerges from the cross-linking of an oxidized Tyr residue with the side chain of a Lys residue. Since PQQ shares the same reactive *ortho*-quinone structure as LTQ, PQQ is capable of catalyzing the same reaction as LOX/LOXLs, namely the oxidative deamination of primary amines. In this process, Cu^{2+} is crucial for the regeneration of the *ortho*-quinone. While LTQ in LOX/LOXL and PQQ go through exactly the same reaction cycle, the latter does not require an enzyme to be reactive (Figure 1A).[23] PQQ-induced cross-linking has been previously demonstrated for elastin polypeptides.[24,25] Here, we utilized PQQ to cross-link recombinant full-length TE, examined the resulting molecular modifications, microstructure, and mechanical properties, and compared them to native elastin. We furthermore introduce a technique for the repeated and thus cost-effective use of PQQ by covalently coupling it to magnetic beads. Our findings show the potential of PQQ for its usage in the cost-effective fabrication of protein-based biomaterials as an alternative to conventional chemical cross-linkers.

2. Results

2.1. PQQ Induces Allysine Formation in Recombinant Tropoelastin

Solutions of recombinant human TE were incubated with PQQ in the presence of divalent copper at elevated temperatures to form a material that is similar to mature elastin in terms of its physicochemical properties and molecular assembly. Proper TE coacervation was assured by incubating at temperatures above 37 °C and an increased ionic strength of the cross-linking buffer.

To investigate the modifications induced by PQQ on the molecular level, we performed HPLC-MS analyses of pancreatic elastase (PE) digests from cross-linked TE (cTE) and determined modified amino acid residues using an untargeted sequencing approach. The sequenced peptides obtained by MS analyses covered 88% and 69% of the human TE sequence (isoform 2, excluding signal peptide) after reaction at 40 and 50 °C, respectively. The majority of the sequence segments that were not recovered by non-cross-linked peptides, especially derived from cTE incubated at 50 °C, were located within KA cross-linking sequences encompassing at least one of the Lys residues. We additionally performed a tryptic digest of a cTE pellet after reaction at 50 °C, for which the sequence coverage from PE digests was rather low, and subjected the supernatant of the incomplete digest to MS analysis. Upon sequencing, we obtained a sequence coverage of 99%. PQQ-induced modifications were identified by screening all cTE digests for allysine (Lya, see Figure 1A for chemical structure) and its oxidation product α-aminoadipic acid (Aad). Altogether, free Lya residues were detected in KP domains 4 (Lys-61, Lys-64), 8 (Lys-137, Lys-140), 10 (Lys-178), 12 (Lys-209, Lys-212), and 13 (Lys-225) as well as in KA domains 6 (Lys-107), 14 (Lys-241), 21 (Lys-451), 23 (Lys-463), 25 (Lys-533, Lys-537), 27 (Lys-591), and 29 (Lys-631). However, a significant amount of Lya residues underwent further oxidation to Aad and were therefore not involved in cross-linking. Virtually all Lys residues found to be partially modified to Lya were also found to be partially oxidized to Aad. Additionally, Lys-261 and Lys-375 of domains 15 and 19, respectively, as well as Lys-673 and Lys-676 of domain 31 were partially modified to Aad. In summary, at least one Lys residue of every cross-linking motif identified in human skin and aortic elastin[12] was found to be partially modified to Lya and/or Aad. As an example, an annotated mass spectrum of a peptide comprising two Lya residues is shown in **Figure 2**A. The analysis of the trypsinized control sample (TE incubated in the absence of PQQ and Cu^{2+})
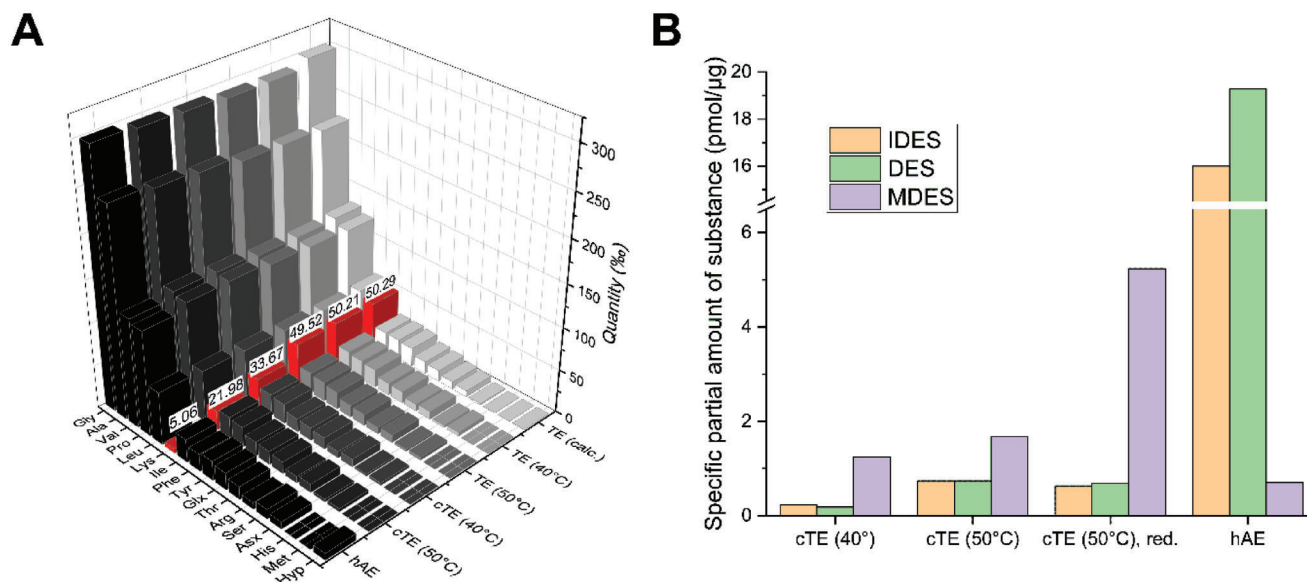
Figure 3. Quantification of free Lys and cross-linking amino acids. A) The results of amino acid analysis are shown for human aortic elastin (hAE), cTE at 40 and 50 °C incubation temperature, and TE control samples incubated at 40 and 50 °C without PQQ/Cu^{2+}. TE (calc.) indicates the expected values calculated from the amino acid sequence of TE isoform 2 (Swiss-Prot AC P15502-2, G422S). Amino acids are depicted by their three-letter code. Values for free lysine are highlighted in red and the quantity in ‰ is indicated above. The addition of PQQ/Cu^{2+} causes a decrease in free lysine which is supported by an increasing incubation temperature. B) The diagram compares the specific partial amounts of substance for the cross-linking amino acids isodesmosine (IDES), desmosine (DES), and merodesmosine (MDES) of cTE incubated at 40 and 50 °C, NaBH$_4$-reduced cTE and hAE. The increase in MDES upon reduction implies a high amount of ΔMDES in cTE. This together with the relatively low amount of DES and IDES indicates a still immature cross-linking of cTE. The reference data for hAE in (A) and (B) is taken from.[12]

yielded a sequence coverage of 98% and confirmed the absence of Lys-derived modifications (Lya, Aad) in the starting material.

2.2. PQQ Mediates an Elastin-Like Cross-Linking Cascade with Recombinant Tropoelastin

The formation of Lya is required to form a cross-linking pattern similar to that of mature elastin. As shown in the previous paragraph, PQQ is capable of catalyzing the oxidation of the same Lys residues in TE as LOX/L does. Two possible types of initial cross-links can emerge from Lya in modified TE. The condensation of Lya and Lys yields the Schiff base cross-link dehydrolysinonorleucine (ΔLNL, Figure 1B) and the aldol condensation of two Lya residues forms the enal-type cross-link allysine aldol (AA, Figure 1B). Based on MS data analysis, both possible types of bifunctional cross-links were identified in cTE. In more detail, the formation of bifunctional intra-domain cross-links was shown for KP domains 4 (ΔLNL, AA), 8 (ΔLNL, AA), 10 (ΔLNL, AA), and 12 (ΔLNL, AA) as well as KA domains 6 (ΔLNL, AA), 15 (ΔLNL), 19 (ΔLNL), 21 (AA), 23 (ΔLNL), and 31 (ΔLNL). Within these cross-linking motifs, the adjacent Lys residues are covalently linked to each other. We further quantified the Lys modification degree by amino acid analysis as depicted in **Figure 3**A. The Lys content of the control samples incubated at 40 and 50°C in the absence of PQQ and Cu^{2+} matches the theoretical Lys content of ≈50‰. However, in the cTE samples, free Lys was reduced by 33% and 56% for incubation temperatures of 40 and 50 °C, respectively. For comparison, only 10% free Lys was detected in mature elastin isolated from human

aorta.[12] Moreover, the analysis of cross-linking amino acids after total hydrolysis of cTE proved the initiation of the cascading formation of higher-functional cross-links (see Figure 1B for their chemical structures and Figure 8 for the cross-linking cascade) in cTE. DES and IDES were detected and quantified as shown in Figure 3B. It is noteworthy that the DES-to-IDES ratio in non-reduced cTE is ≤1.0, whereas DES is slightly more abundant in mature human elastin than IDES.[12] This is consistent with results obtained by Bellingham et al.[24] on the PQQ-induced cross-linking of elastin-like polypeptides. In addition to tetrafunctional cross-links, we were also able to detect the trifunctional cross-linking amino acid MDES by amino acid analysis. The referring peak assigned as MDES was eluting between DES and LNL that is consistent with chromatograms published by Francis et al.[26] and Bellingham et al.[24] and was verified by a series of experiments. Elastin from porcine arteries and bovine *ligamentum nuchae* was isolated by collagenase treatment with subsequent NaOH extraction. The signal assigned to MDES was strongly present in both collagenase-treated and NaOH-extracted pellets and therefore relates to an amino acid released from elastin. Its intensity increased after NaBH$_4$ reduction prior to collagenase treatment, which is a result of conversion of dehydromerodesmosine (ΔMDES, Figure 1B) to MDES in cTE. Like the signals of IDES, DES, and LNL, the assigned MDES signal was almost absent in the supernatant of NaOH extraction. The analysis of this signal revealed a remarkable amount of MDES in cTE hydrolysates that increased when the cTE samples were previously reduced by NaBH$_4$. This indicates that the majority of the trifunctional cross-links are present as ΔMDES but also gives evidence for the presence of reduced

**ADVANCED
SCIENCE NEWS**

www.advancedsciencenews.com

**[M]acro-olecular
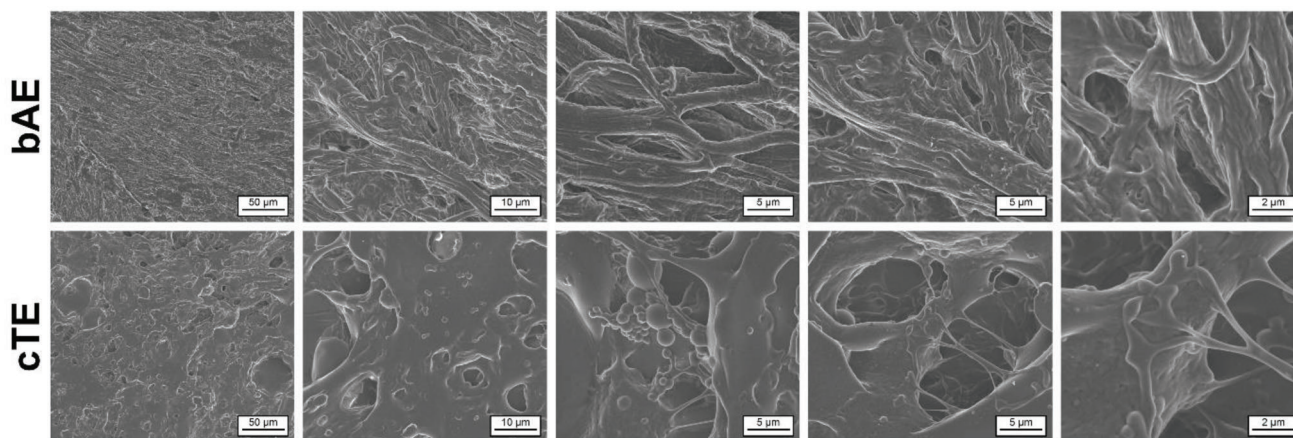Bioscience**

www.mbs-journal.de

Figure 4. Microstructure of mature elastin and cTE. The upper panel shows the microstructure of mature bovine aortic elastin (bAE). A network of distinct and oriented elastin fibers, that is, elastic fibers without the fibrillin mantle, is visible. cTE (lower panel) is characterized by a more amorphous but also porous microstructure. Bulky regions are occasionally spanned by short fibrillar structures. Globular structures are artefacts of coacervated tropoelastin.

MDES in cTE in the absence of externally added hydrogenation agents.

2.3. Morphological Characterization of cTE

The microstructure of cTE was analyzed by scanning electron microscopy (SEM) and compared to isolated bovine aortic elastin (bAE) as a reference. Whereas bAE shows a clear fibrous structure (**Figure 4**, upper panel), cTE possesses a rather amorphous, yet porous morphology (Figure 4, lower panel). Higher magnification reveals short fibril-like shapes that span between bulky amorphous areas in cTE. However, those structures differ substantially in length, diameter, and shape from the fibrils in mature elastin. Spherical structures in cTE are a result of the coacervation process. The formation of spherical TE aggregates is known from previous analyses of cross-linked TE-derived materials.[27,28]

2.4. Mechanical Properties of cTE

The mechanical properties were determined by nanoindentation of three cTE replicates using an atomic force microscope (AFM) and compared to isolated elastin from the bovine neck ligament. Measurements were done in phosphate-buffered saline (PBS), and data were acquired over a sample area of 4 µm^2 with a resolution of 256×256 measurements that were equally distanced. The results are summarized in **Figure 5**A, which shows the histograms of Young's moduli together with the graphs of the Kernel fit function. The Young's moduli are unequally distributed among the three cTE replicates with cTE 1 and 2 showing comparable means and variations whereas the mean and variation of cTE 3 are shifted toward higher values. When compared to elastin, the distribution of Young's modulus in cTE 3 is closest to that of native elastin but all cTE histograms are overlapping with the elastin histogram. The box plot representation of the data in Figure 5B shows the upper and lower quartile, mean and median values as well as the standard deviation. The mean Young's

modulus was determined to be 1.755 ± 0.312 MPa for elastin, 1.006 ± 0.134 MPa for cTE 1, 1.207 ± 0.116 MPa for cTE 2, and 1.930 ± 0.241 MPa for cTE 3. A Tukey post-hoc test shows that the means of all cTE samples differ significantly from that of elastin and are also significantly different from each other among the cTE samples ($\alpha = 0.001$, p $= 2.22 \times 10^{-16}$).

cTE shows elevated resistance against trypsin. Trypsin is a protease that hydrolyzes peptide bonds exclusively C-terminal to Arg and Lys residues unless these are followed by a Pro residue. This characteristic makes it the far most commonly used protease in proteomics. TE possesses only a few Arg residues and ≈90% of its Lys moieties are involved in cross-linking when polymerized to mature elastin. Therefore, elastin is resistant to tryptic proteolysis, and the incubation of cTE with trypsin can indirectly provide further information on the degree of cross-linking and the materials' integrity. After 24 h of incubation with trypsin, the mass of the cTE pellet lowered less than 10%. The comparison of peptide profiles of tryptic digests from cTE and soluble tropoelastin (**Figure 6**) revealed that virtually no peptides were released from the cTE digest. This indicates a highly elevated resistance of cTE against trypsin and supports the findings obtained on the rate of Lys modification.

2.5. Several Reaction Cycles Can Be Achieved with Immobilized PQQ

We functionalized magnetic Sepharose beads with PQQ and performed repeated reaction cycles with peptide and protein targets. The MALDI-TOF mass spectra depicted in **Figure 7** show the signals of the synthetic precursor peptide derived from TE domain 19 and cross-linked species for the initial experiment and the first repetition using the same batch of PQQ beads. The signals detected at higher m/z values are absent in the spectrum when the peptide was not incubated with PQQ/Cu^{2+}. The third reaction cycle was performed with TE as the target molecule. The MS/MS analysis of proteolytic digests of the resultant material indicated modified Lys residues in KP domains 4 (Lys-64), 8 (Lys-140), and
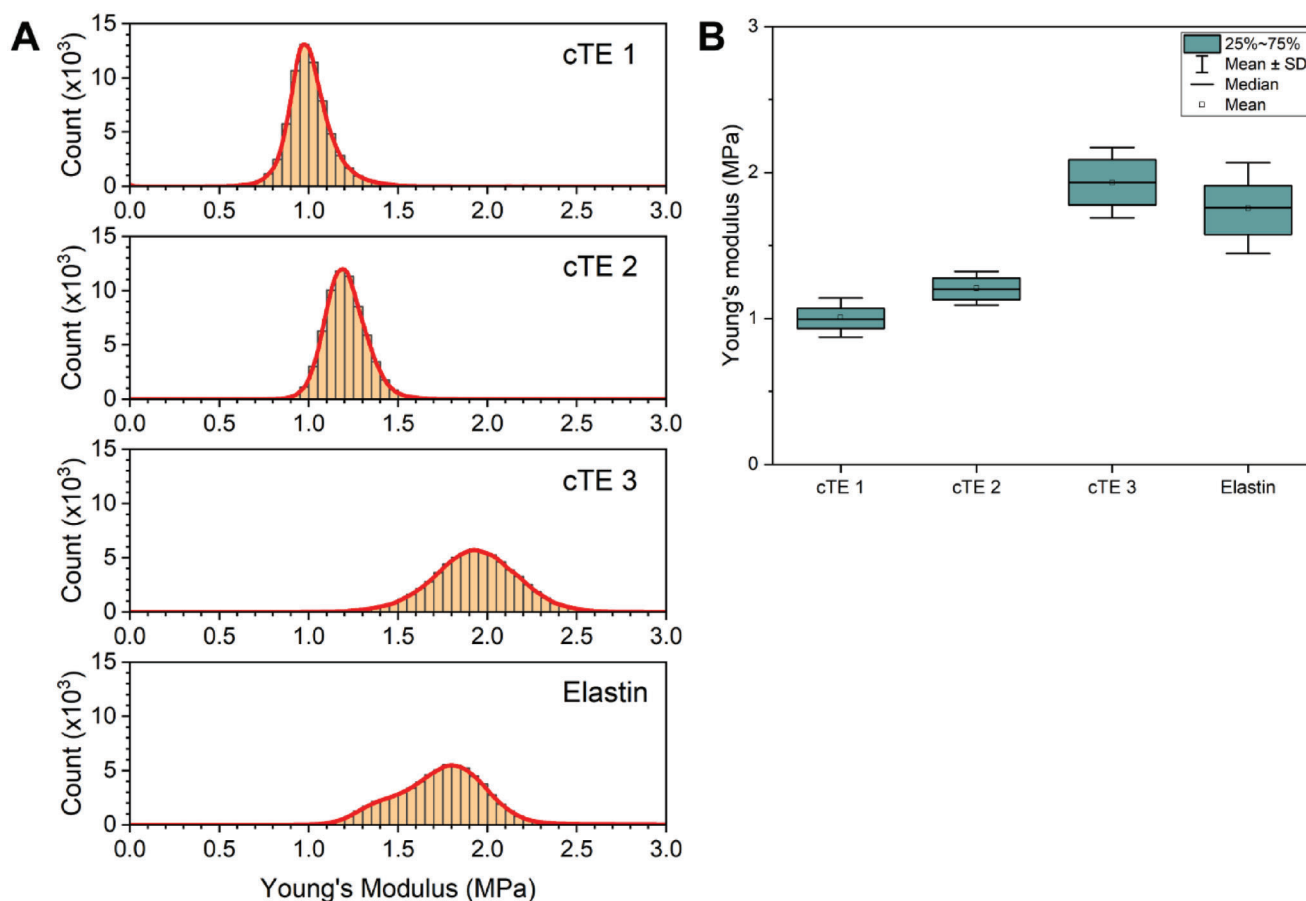
**ADVANCED
SCIENCE NEWS**

www.advancedsciencenews.com

Macro-
molecular
Bioscience

www.mbs-journal.de

Figure 5. Mechanical properties of cTE. A) Histograms of Young's modulus from three cTE replicates and bovine neck ligament elastin determined by AFM nanoindentation are shown in orange. The Kernel fit curve for each histogram is shown in red. The mean Young's moduli of the three cTE replicates lie between 1 and 2 MPa and span across the distribution of Young's modulus of the elastin reference. B) Box plot representation of the data acquired by AFM nanoindentation. Tukey post-hoc analysis indicates that the mean Young's moduli from all cTE replicate significantly differ from each other and that of elastin ($\alpha = 0.001$, p $= 2.22 \times 10^{-16}$). The results indicate elastin-like properties but heterogeneous mechanical properties among different cTE batches.

12 (Lys-212) as well as in KA domains 6 (Lys-107), 15 (Lys-265), 25 (Lys-534), 27 (Lys-594), and 31 (Lys-676). As described for the analyses with free PQQ, we were able to identify both Lya and Aad. Domain 8 was identified to be internally cross-linked via ΔLNL.

3. Discussion

Biomaterial research and design are frequently focused on elastin-like polypeptides and tropoelastin to develop materials that resemble the physicochemical properties of elastin in biomedical applications.[18,29] Elastin's properties are based on its unique molecular structure and assembly. As reviewed elsewhere, this structure is also the basis for alternative approaches to producing elastin-like biomaterials, for example, from elastin-like peptides or elastin-like recombinamers.[30,31] However, genetic engineering nowadays also allows the recombinant production of many natural proteins, such as the monomeric elastin precursor protein TE. As we have recently shown in two different studies of bovine and human elastin,[11,12] mammalian elastin possesses a rather randomized cross-linking pattern, which was

evident by the identification of distinct Lys residues being involved in various types of cross-links or even remained unaltered.

To our best knowledge, this is the first study describing PQQ-induced cross-linking of full-length TE. As mentioned, we have performed enzymatic in vitro cross-linking of recombinant full-length TE using recombinant human LOXL2, which also resulted in an insoluble, partially cross-linked, and elastic biomaterial.[10] Both materials showed elevated resistance against proteolytic cleavage by trypsin whereby this feature was clearly more pronounced with PQQ-treated cTE. Compared to human aortic elastin (hAE), the reduced modulus (E*) of LOXL2-cross-linked cTE was 34% higher (E*(cTE) = 193.1 ± 13.9 kPa vs E*(hAE) = 144.2 ± 10.8 kPa).[10] In the present study, we compared three PQQ-cross-linked cTE samples with native elastin extracted from bovine *ligamentum nuchae*. Here, we saw overlapping histograms but significant deviations from the mean Young's modulus on both sides. In general, Young's moduli for PQQ-cross-linked cTE ranged between 1 and 2 MPa. Overall, the results indicate elastin-like properties of cTE but heterogeneous mechanical properties among different cTE batches. In literature, Young's modulus of elastin fibers is reported to be 1.2 MPa.[32]
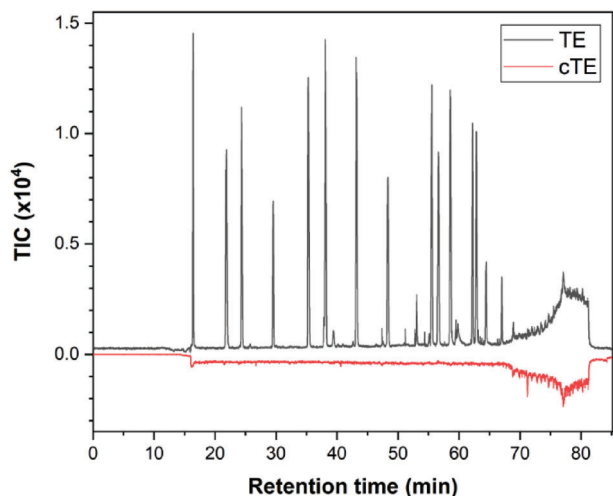
Figure 6. Peptide chromatograms from tryptic tropoelastin and cTE digests. The total ion current (TIC) chromatograms of peptides released from tryptic digests of solubilized tropoelastin (dark gray) and immersed cTE (red) were acquired by HPLC-MS after 250-fold dilution. This figure indicates a strongly decreased susceptibility of trypsin to cTE as barely any signals are detectable in the cTE digest.

HPLC-MS-based molecular analysis of proteolytically digested cTE showed a decreased sequence coverage with significant gaps around the cross-linking motifs of KA domains. Similar results are obtained in analyses of isolated mature elastin and indicate the involvement of the referring Lys residues in cross-linking. However, it must be considered that this interpretation is biased by a cleavage preference of PE in oligo-Ala sequences[33,34] that may produce very short unassignable peptides. Peptide sequencing revealed the PQQ-induced oxidative deamination of Lys residues in every cross-linking domain of TE evident by the identification of Lya and Aad. It is noteworthy that the relative abundance of Aad may indicate a directed formation, which is discussed below. For all KP- and most KA-type cross-linking motifs with more than one Lys residue, at least one cross-linked peptide was identified. The cross-linked peptides identified in this study are internally cross-linked forming a cyclic structure through the former Lys side chains. For elastin and TE-based materials, this implies the covalent linkage of two adjacent Lys residues within a single cross-linking domain. These types of cross-links were also identified in mature human and bovine elastin,[11,12] which proves that they do not only serve as intermediates in the formation of the higher-functional DES and IDES cross-links but exist alongside. As intra-domain cross-links are only capable of stabilizing local secondary structural elements, their overall contribution to the stability of elastin and elastin-like biomaterials may be limited. Bifunctional interconnections between Lys residues of different domains have not been identified in this study. Regarding the close proximity of pairwise Lys residues in KA- and KP-type cross-linking domains of TE, the formation of intra-domain cross-links seems to be kinetically favored over the formation of inter-domain linkages. When compared to mature human elastin, the frequency of pairwise Lys residues internally connected by AA was remarkably higher relative to the total number of identified internally cross-linked peptides. This increase in
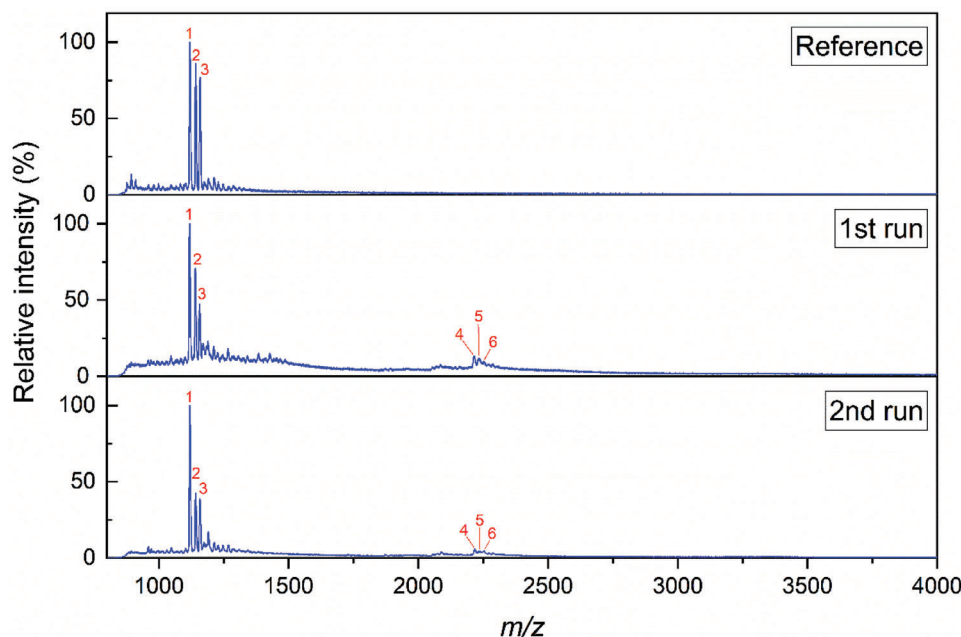

Figure 7. MALDI-TOF mass spectra from peptide samples incubated with PQQ-modified beads. The spectra show the results of MALDI-TOF analyses from a peptide cross-linking assay that was done with a single batch of PQQ-modified magnetic Sepharose beads. The reference graph refers to the peptide with the sequence H_2N-AAKAAAKAAKYG-NH_2. The assigned signals 1, 2, and 3 relate to the singly protonated peptide species, the sodium, and potassium adducts, respectively. After the first incubation of the peptide solution with PQQ-modified beads, three signals assigned to numbers 4, 5, and 6 were detected between m/z 2219 and 2257, which correspond to the singly protonated peptide dimer cross-linked by ΔLNL as well as their sodium and potassium adducts. The same signals were detected after a repetition of this experiment with the same batch of PQQ-modified beads.
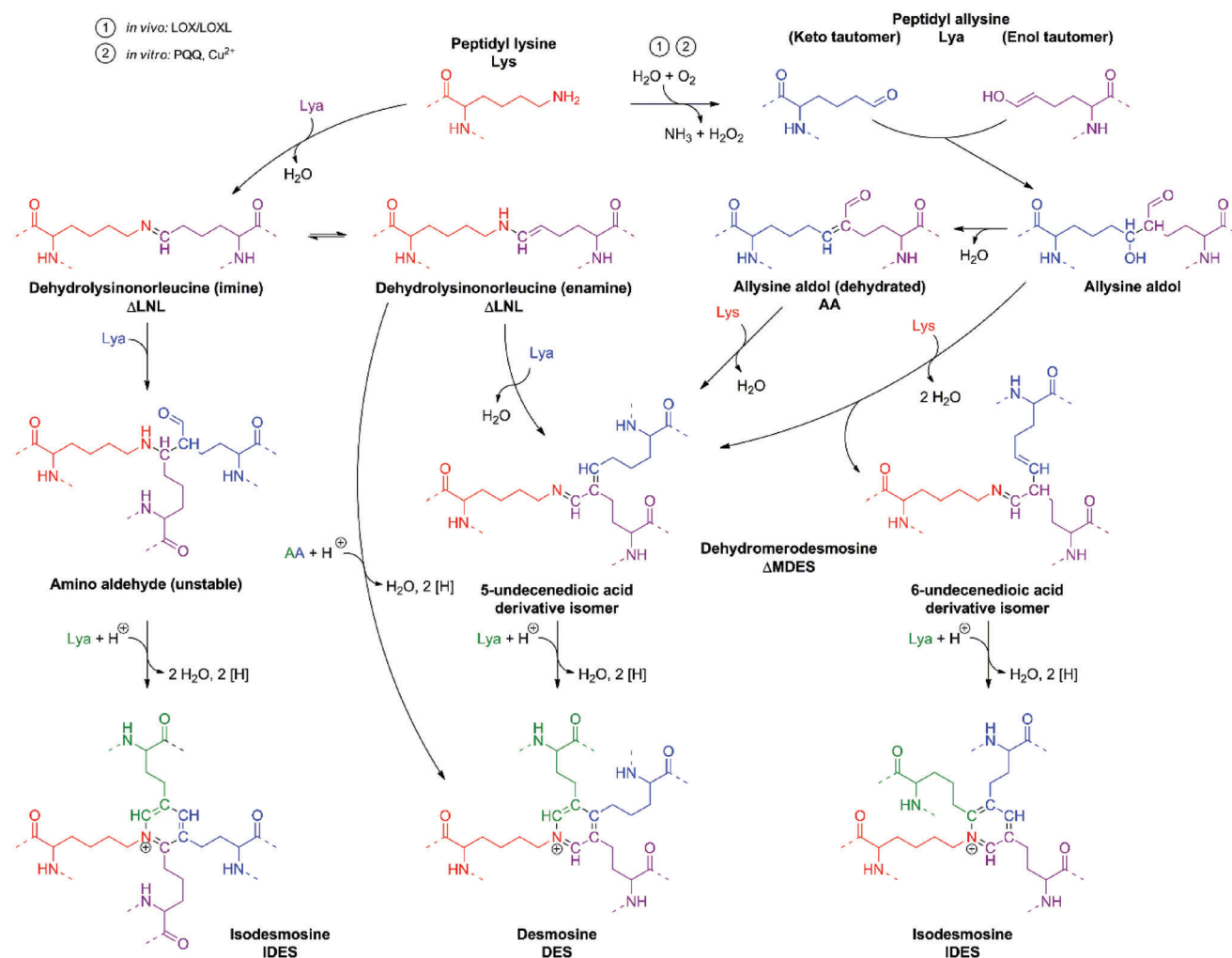
**ADVANCED
SCIENCE NEWS**

www.advancedsciencenews.com

**Macro-
molecular
Bioscience**

www.mbs-journal.de

Figure 8. Pathways of sequential cross-linking in elastin and cTE. Peptidyl lysine (Lys) is oxidatively deaminated to allysine (Lya) by LOX/LOXL in vivo or PQQ/Cu^{2+} in vitro. ΔLNL is formed by the condensation of Lys and Lya. Further condensation involving Lya residues yields IDES via the unstable amino aldehyde intermediate or DES via ΔMDES or direct condensation with dehydrated AA. AA is formed by the aldol reaction of two Lya residues. Subsequent water elimination will form dehydrated AA, in literature also known as "aldol condensation product" (ACP). Hydrated AA can form two isomers of ΔMDES upon condensation with Lys that either result in the formation of DES or IDES upon condensation with a further Lya moiety. The individual former Lys side chains that compose the cross-linking structures are indicated in orange, blue, purple, and green. This scheme summarizes reaction pathways published in references.[36,38–42]

observed AA cross-linked peptides requires an overall increased presence of Lya in cTE over elastin. Shah et al. investigated the PQQ-mediated oxidation of peptidyl lysine in insoluble, immature elastin from embryonic chicken aortas and compared it to the LOX-induced modifications.[35] The authors showed a conspicuous increase in Lya upon incubation with PQQ/Cu^{2+}, which was even higher when compared to LOX-treated elastin. However, the amounts of cross-linkages increased less than in LOX-treated elastin. Together with the results that we report here, this is an indication of a reduced efficiency in cross-linking with PQQ that might be caused by further oxidation of Lya to form Aad. This reduces the overall number of reactive sites for cross-link formation and explains an overall reduced degree of cross-linking when compared to LOX. The formation of Aad might be directly coupled to a possible side reaction of PQQ as discussed later.

Although we were not able to verify bifunctional linkages between different domains in cTE by mass spectrometry, the detection and quantification of higher functional cross-links by amino acid analysis prove the formation of inter-domain linkages. The tetrafunctional cross-linking amino acids DES and IDES are formed from the bifunctional intermediates ΔLNL and AA by further condensation reactions and thereby connect at least two different domains. In comparison to mature elastin, the amount of DES and IDES in cTE was 24× lower. This circumstance may be related to the kinetics of the formation of 1,2-dihydropyridine cross-links (unoxidized precursors of DES/IDES), which is considered to be a reaction of third order in a protein-free model system investigated by Davis and Anwar starting from ΔLNL analogs.[36] Additionally, cTE does not contain hydroxyproline since the TE was produced recombinantly by prokaryotic cells. It has been shown that hydroxyproline has an
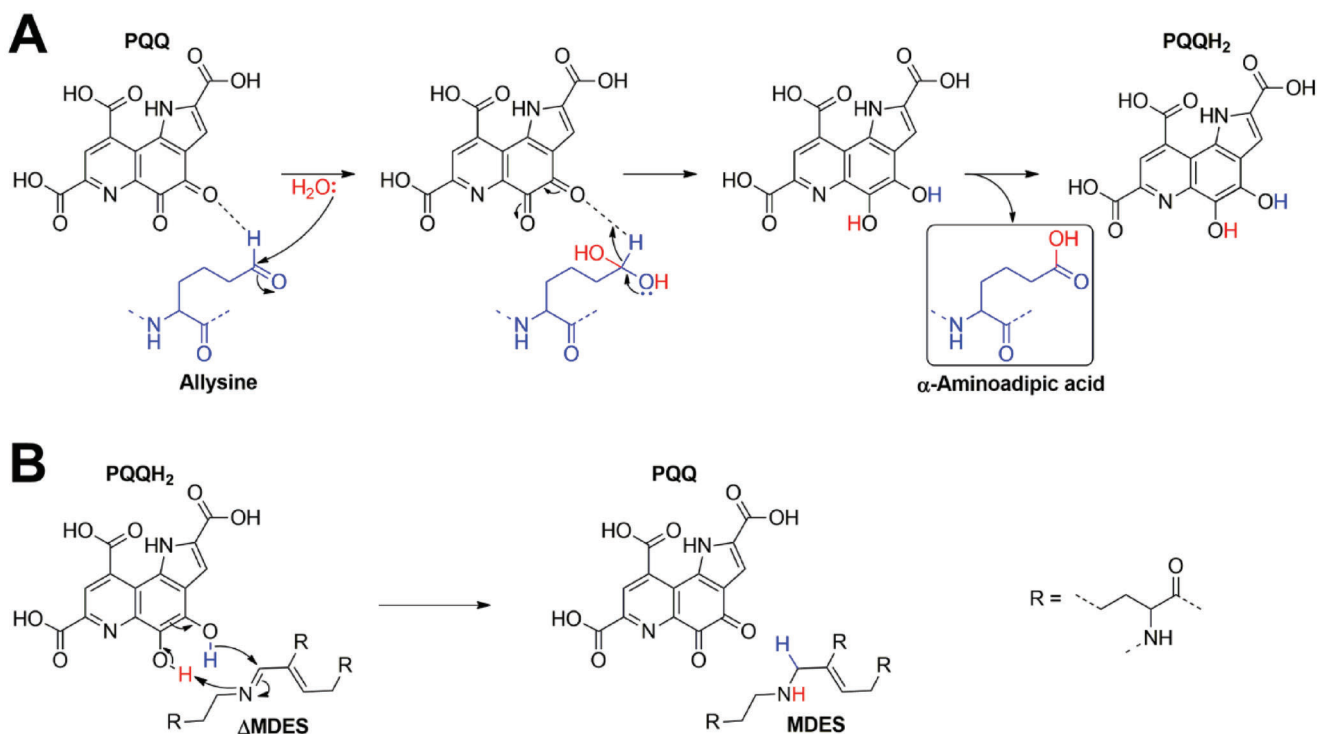
**ADVANCED
SCIENCE NEWS**

www.advancedsciencenews.com

**Macro-
molecular
Bioscience**

www.mbs-journal.de

Figure 9. Proposed pathways of PQQ-mediated allysine oxidation and ΔMDES reduction. A) PQQ-mediated allysine oxidation is initiated by aldehyde hydration to form a geminal diol intermediate. Subsequent electron pair rearrangements and proton abstraction release α-aminoadipic acid and pyrrolo-quinoline quinol (PQQH$_2$). The water molecule and allysine as well as the respective descended species are colored red and blue, respectively. B) PQQH$_2$ transfers two protons and an electron pair to ΔMDES to release MDES and reoxidized PQQ. The transferred hydride is depicted in blue, the proton is colored red.

effect on the coacervation behavior of elastin-like peptides,[37] and its absence will therefore most likely influence the coacervation of TE and the subsequent PQQ-mediated cross-linking in cTE. Nevertheless, considering pyridine cross-link formation in a protein, kinetics is in addition significantly influenced by backbone movement, which is required to bring two or more cross-linking domains in close proximity resulting generally in a shift to lower rate constants. It is therefore expected that the content of tetra-functional cross-linking amino acids will increase over time and may alter the characteristics of cTE. This is especially supported by the detection of MDES in cTE and NaBH$_4$-treated cTE. NaBH$_4$ treatment leads to a threefold increase in the amount of MDES indicating a major amount of ΔMDES in cTE that is capable of further condensing with Lya to form DES and IDES according to the pathways shown in **Figure 8**. When compared to elastin from human tissues the DES-to-IDES ratio is lower in cTE meaning a relatively higher amount or even a preferred formation of IDES. This observation is consistent with a study by Bellingham et al. on the PQQ-induced cross-linking of elastin-like polypeptides.[24]

According to the pathways of sequential cross-linking shown in Figure 8, the unstable amino aldehyde and the 6-undecenedioic acid-type of ΔMDES may in vitro be more preferably formed intermediates from ΔLNL and AA, respectively. Unlike the amino aldehyde intermediate, ΔMDES is a stable cross-linking structure and can be detected by amino acid analysis upon reduction of the Schiff base linkage to form MDES. Without reduction, ΔMDES would decompose during

total hydrolysis to release a free Lys residue and aldosine, a hydrolysis product of AA.[43] Considering this, it is worth mentioning that the ratio of free Lys in the non-reduced cTE samples may be slightly shifted to higher values due to the release of free Lys from ΔMDES. However, like Bellingham and coworkers,[24] we also detected MDES in samples that were not treated with NaBH$_4$. This implies a pathway of redox side reactions that generate reduced PQQH$_2$ during the incubation of the samples. Although Bellingham et al. did not discuss this finding, it is of relevance in the context of our results that detected high amounts of Aad by mass spectrometry since both findings can be explained by the proposed pathway of a side reaction as depicted in **Figure 9**. The therein proposed PQQ-mediated oxidation of Lya to Aad leads to the formation of PQQH$_2$, which is potentially capable of reducing ΔMDES. The PQQ-mediated oxidation of aldehydes is already described in the literature. Membrane-bound PQQ-dependent enzymes that transform formaldehyde to formate, which is essentially the same type of chemical transformation, were identified in prokaryotes.[44,45] However, it has also been shown that PQQ is capable to transform acetaldehyde in a non-enzymatic reaction at elevated temperatures.[46]

Overall, we have demonstrated the fabrication of an artificial insoluble elastin based on full-length TE that is matured by PQQ-induced cross-links known from native elastin. By coupling PQQ covalently to magnetic beads, we showed its reusability in an enzyme-like manner. In the context of collagen- and

elastin-related biomaterial research, PQQ is a suitable substitute to common Lys-reactive cross-linkers like carbodiimides, NHS esters, or aldehydes and compensates for the lack of recombinant LOX or related enzymes.

4. Experimental Section

PQQ, sodium chloride, N-hydroxysuccinimide (NHS), hydroxylammonium chloride, α-cyano-4-hydroxycinnamic acid, copper sulfate pentahydrate, collagenase, and sodium borohydride were purchased from Sigma Aldrich (Steinheim, Germany). 1-Ethyl-3-(3-dimethylaminopropyl)carbodiimide hydrochloride (EDC ∎ HCl), 2-(N-morpholino)ethanesulfonic acid (MES), acetic acid, formic acid (FA), acetonitrile (ACN), ethanol (EtOH), and monobasic potassium phosphate were obtained from Carl Roth (Karlsruhe, Germany). Invitrogen Dynabeads M-270 Amine and Pierce trypsin protease were bought from Thermo Fisher Scientific (Karlsruhe, Germany). Porcine pancreatic elastase was obtained from Elastin Products Company (Owensville, MO, USA). Dibasic sodium phosphate, 2-amino-2-(hydroxymethyl)propane-1,3-diol (Tris), potassium dihydrogen phosphate, dipotassium hydrogen phosphate, hydrochloric acid, and iron(III) chloride hexahydrate were bought from Merck (Darmstadt, Germany). Trifluoroacetic acid was obtained from Fluka (Munich, Germany). The peptide H$_2$N-AAKAAAKAAKYG-NH$_2$ was synthesized by the Department of Drug Design and Target Validation of the Fraunhofer Institute for Cell Therapy and Immunology IZI (Halle (Saale), Germany). Unless otherwise stated, double-distilled water (ddH$_2$O) was used as a solvent. All other chemicals were also purchased from Carl Roth GmbH & Co. KG (Karlsruhe, Germany).

Expression Vector and Host Strain: The DNA sequence of human TE (isoform 2, GenBank entry: AAC98394, amino acid 27–724) with optimized codon usage for E. coli was obtained from the Thermo Fisher Scientific GENEART GmbH (Regensburg, Germany) and was inserted into Novagen´s vector pET-28a(+) (Merck KGaA, Darmstadt, Germany) via NcoI and BamHI. The cer site of the natural plasmid ColE1[47] was inserted into the vector via SphI . For expression of TE (IF 2) the E. coli strain BL21-Gold (DE3) (B F- ompT hsdS(rB- mB-) dcm+ Tetr gal λ(DE3) endA Hte) from Agilent Technologies Germany GmbH & Co. KG (Waldbronn, Germany) was used as host.

Protein Production and Purification: For TE (IF 2) production, cells were grown in M9 minimal medium (pH 7.1) containing 8.95 g L^{-1} Na$_2$HPO$_4$ x 2 H$_2$O, 3.4 g L^{-1} KH$_2$PO$_4$, 0.58 g L^{-1} NaCl, 2.95 g L^{-1} NH$_4$Cl, 2 mL L^{-1} trace elements,[48] 1.2 g L^{-1} MgSO$_4$ x 7 H$_2$O, 20 g L^{-1} glucose, and 50 mg L^{-1} kanamycin (only in pre-cultures). The fermenter Biostat C 30 L (B. Braun International GmbH, Germany) was used for TE production in a total volume of 12 L. Cells were cultivated at 37 °C and initial aeration of 4.5 L min^{-1}. The pO$_2$ was set constant at 25% regulated by aeration and stirrer speed cascade. The pH value was regulated to 7.1 by using 20% (v/v) H$_3$PO$_4$ and 25% (v/v) NH$_3$ solution. The TE production was induced at OD ≈16 with 1 mM IPTG. Glucose concentration was measured by using the glucose analyzer YSI 2700 Select (YSI Inc., USA). The feed solution contained M9 minimal medium with 500 g L^{-1} glucose. A feed pulse of 10 g L^{-1} glucose was added when a glucose concentration lower than 5 g L^{-1} was reached. Cells were harvested after 2 h induction phase and were stored at −20 °C.

For TE extraction, 100 g of frozen E. coli bio wet mass was heated in a microwave oven (NN-SD452W, Panasonic, Kadoma, Japan) at 1000 W in 15 sec intervals to >70 °C to inactivate host cell proteases. The heated bio wet mass was suspended in 300 mL of cold 10 mM ammonium acetate buffer (pH 6.7) and was homogenized at 10 000 rpm using an Ultra-Turrax Miccra R-T D-1 (ART moderne Labortechnik, Mühlheim, Germany). Cells were disrupted in high-pressure homogenizer APV-2000 (APV-systems, Albertslund, Denmark) at 1000 bar for three passages with cooling on ice between each passage. The cell lysate was centrifuged at 17 000 g for 30 min at 4 °C by using Avanti J-30i (Beckman Coulter GmbH, Krefeld, Germany). The soluble fraction was decanted, and the pellet was washed in 300 mL

of cold 10 mM ammonium acetate buffer (pH 6.7). All the following steps were performed at an ambient temperature of ≈21 °C. TE was extracted from the insoluble fraction by stirring in a 300 mL extraction mixture containing 70% acetone, 20% 250 mM ammonium acetate buffer (pH 5.0), and 10% ddH$_2$O for 4 h. The soluble, TE-containing fraction was received via centrifugation at 17 000 g for 10 min. The extraction step was performed three times in total. Acetone was removed from three pooled supernatants by using a rotary evaporator HeidolPh2 (Heidolph Instruments GmbH & Co. KG, Schwabach, Germany) at 25 °C water bath temperature and vacuum pressure down to 15 mbar. Soluble TE was exhaustively dialyzed against ultrapure water (total dilution 1:10 000), was freeze-dried using Lyovac GT 2-E (Steris, OH, USA) at 0.22 mbar vacuum pressure, and was stored at −20 °C.

In vitro Cross-Linking of TE: TE, PQQ, and copper sulfate were dissolved in cross-linking buffer (50 mM Tris-HCl, 150 mM NaCl, pH 8.5) at final concentrations of 10 mg mL^{-1}, 4 mM, and 2 mM, respectively. TE was incubated at 40 °C for 5 min prior to adding PQQ and copper sulfate to allow coacervation to occur. Subsequently, the temperature was kept constant at 40 °C or raised to 50 °C. All samples were incubated for 24 h. Negative controls were run under identical conditions without adding PQQ/Cu^{2+}. All samples were incubated in a Thermomixer (Eppendorf AG) at 350 rpm. After 24 h, the samples were centrifuged for 5 min at 14 100× g, the supernatant was removed, and the pellets were rinsed with ddH$_2$O, 1:1 (v/v) EtOH/ddH$_2$O and pure EtOH and dried under laminar flow.

Enzymatic Digests and Mass Spectrometric Analysis: Cross-linked TE (cTE) pellets were dispersed in 50 mM Tris-HCl (500 µL buffer per mg pellet) and digested with pancreatic elastase in an enzyme-to-substrate ratio of 1:50 (w/w) for 24 h at 37 °C. The reaction was afterward quenched by adding 0.5% (v/v) TFA. The peptide solutions were desalted with C18-ZipTips according to the manufacturer's protocol and analyzed by reversed-phase high-performance liquid chromatography (HPLC) coupled with high-resolution mass spectrometry (MS). The peptides were separated on an EASY-nLC 1000 HPLC system (Thermo Fisher Scientific) with 0.1% (v/v) FA in ddH$_2$O and 0.1% (v/v) FA in ACN as solvents A and B, respectively. The peptides were washed on a trap column (Acclaim PepMap 100 trap-column 75 µm × 2 cm, nanoViper, C18, Thermo Fisher Scientific) for 15 min at 100% A and subsequently transferred to the separation column (EASY-Spray column, 50 cm × 75 µm ID, PepMap C18, 2 µm, Thermo Fisher Scientific). Peptides were eluted by applying an increasing gradient of solvent B from 5% to 40% within 120 min at a flow rate of 300 nL min^{-1}. The outlet of the HPLC system was online-coupled to an Orbitrap Q Exactive Plus mass spectrometer (Thermo Fisher Scientific). The capillary voltage was adjusted between 1.8 and 2.5 kV for a stable electrospray. Precursor ions were acquired from m/z 400 to m/z 2000 at a resolution of 75 000. The 10 most abundant species were selected for higher energy collisional dissociation (HCD) at 28% normalized collisional energy. The isolation window was set to 1.5 Th. Fragment ions were detected from m/z 120 to m/z 1800 at a resolution of 17 500. Dynamic exclusion with a mass tolerance of 2 ppm was applied for 40 s.

Tryptic digestion of cTE was done by dispersing 795 mg of cTE in 500 µL 50 mM ammonium bicarbonate buffer (pH 8.0). Trypsin was added at an enzyme-to-substrate ratio of 1:100 (w/w), and the digestion was performed as previously described. The pellet was subsequently dried and weighed. A TE solution of the same concentration was trypsinized in the same way as the cTE pellet. The supernatants of the cTE digest and the digested solubilized TE were 200× diluted and subsequently analyzed by HPLC-coupled quadrupole-time of flight mass spectrometry (QTOF MS). Diluted sample (2.5 µL) was injected on an Ultimate 3000 RSLCnano HPLC device (Thermo Fisher Scientific) equipped with a reversed-phase trap column (Acclaim PepMap 100 C18, 3 µm, 100 Å, 300 µm ID × 5 mm; Thermo Fisher Scientific) and separation column (Acclaim PepMap RSLC C18, 2 µm, 100 Å, 75 µm ID x 150 mm; Thermo Fisher Scientific). FA (0.1% (v/v)) in ddH$_2$O and FA (0.1% (v/v)) in an 80:20 (v/v) mixture of ACN and ddH$_2$O were used as solvents A and B, respectively. Peptides were trapped for 9 min at 100% A and subsequently transferred to the separation column. Peptides were eluted by increasing the concentration of B from 12% to 40% within 60 min. Eluting peptides were detected by online-coupled QTOF MS (Q-TOF-2, Waters/Micromass). Peptides were only detected in

**ADVANCED
SCIENCE NEWS**

www.advancedsciencenews.com

**Macro-
molecular
Bioscience**

www.mbs-journal.de

full scan mode from *m/z* 40 to *m/z* 1550 with a scan time of 1 s. Cone and capillary voltages were set to 25 and 1.9 kV, respectively. The undiluted tryptic digest of cTE was additionally analyzed on the Q Exactive Plus instrument as described above.

Sequencing of Non-Cross-Linked Peptides: Peptides were identified using the software PEAKS Studio, version 7.5 (Bioinformatics Solutions Inc.). The MS data were loaded in raw format and refined with the precursor mass correction option. Automated de novo sequencing was run followed by matching the results to the human subsection of the Swiss-Prot database with the sequence of the recombinant TE included (TE isoform 2, Swiss-Prot AC P15502-2, with residue exchange G422S). Precursor mass tolerance was set to 8 ppm for precursor ions and 15 mDa for product ions. Enzyme specificity was set to "none" for PE digests. For tryptic digests, the enzyme specificity of trypsin was enabled allowing a maximum of three missed cleavages per peptide and non-specific cleavage sites at both ends of the peptide. For all sequencing runs including TE control, α-aminoadipic acid (Lys+14.9633 Da), allysine (Lys-1.0316 Da), and deamidation of Asn and Gln (+0.9840 Da) were included as variable post-translational modifications (PTMs). For data evaluation, the peptide score threshold was adjusted to obtain a false discovery rate of $\leq$1% based on peptide spectrum matches.

Sequencing of Cross-Linked Peptides: Intra-domain cross-links were identified by searching the MS data against a customized database in PEAKS Studio 7.5 as previously described.[11] Briefly, each cross-linking motif was reduced to one single Lys residue, and the missing sequence was defined as PTM together with the cross-linker. Thus, intra-domain cross-links were identified as PTMs and manually validated. Moreover, StavroX (version 3.5.1)[49] was used to identify intra- and inter-domain cross-links. For this, MS raw data were converted to the Mascot generic file format using PEAKS Studio and loaded together with the FASTA sequence of human TE IF 2 (G422S) into StavroX. Data were analyzed for AA, ΔLNL, and LNL cross-links in separate runs. Proposed cross-links were manually evaluated and verified.

Amino Acid Analysis and Cross-Link Quantification: cTE incubated at 40 and 50 °C was subjected to amino acid analysis and cross-link (DES, IDES, merodesmosine (MDES)) quantification together with respective control samples of recombinant TE incubated in the absence of PQQ and Cu^{2+}. For 50 °C incubation temperature, a second cTE sample was prepared as described in the referring section above followed by an additional reduction with $NaBH_4$ to prevent acid-catalyzed hydrolysis of Schiff base linkages (25 mg $NaBH_4$/mL in 0.05 M NaH_2PO_4/0.15 M NaCl pH 7.4, 1 h on ice, 1.5 h at RT). All samples were submitted to acidic hydrolysis in 6 N HCl for 24 h at 110 °C for subsequent amino acid analysis. Common amino acids were separated from cross-linking amino acids to the greatest possible extent by using Bond Elut Cellulose columns (300 mg, Agilent Technologies, Santa Clara, CA, USA). The eluates were dried and redissolved in sodium citrate buffer (pH 2.2). The separation and quantification of cross-linking amino acids were performed on a Biochrom 30 amino acid analyzer (Biochrom) by applying a step gradient to a cation exchange separation column (250 mm × 4.0 mm, 5 µm) with post-column ninhydrin derivatization. The elution comprised the following steps: 5 min sodium citrate buffer (pH 4.25), 40 min sodium citrate buffer (pH 5.35), and 20 min sodium citrate/borate buffer mixture (pH 8.6). The flow rate was held at 15 mL h^{-1} and temperature at 85 °C. The retention times of cross-linking amino acids were verified by corresponding standards. Color factors and leucine as external standards were used for quantification. The position of the assigned MDES peak in the chromatogram is consistent with the report of Francis and coworkers[26] and was verified by a series of experiments in order to rule out possible contaminations from non-elastin proteins or artificial modifications derived from the sample preparation. Briefly, elastin was isolated from bovine *ligamentum nuchae*, porcine aorta, and porcine renal artery by digesting the samples two times with highly purified collagenase (Sigma Aldrich C0773; 100 U mL^{-1}, 37 °C, 18 h). The residual fraction was extracted by hot alkali (0.1 N NaOH, 95 °C, 45 min). The pellets remaining after collagenase digest and NaOH extraction as well as the supernatant from NaOH extraction were subsequently analyzed for cross-linking amino acids as described. This procedure was repeated with samples reduced by $NaBH_4$ prior to collagenase treatment.

The analysis of non-cross-linking amino acids was performed according to a standard protocol supplied by Biochrom.

Scanning Electron Microscopy: The morphologies of cTE and bovine aortic elastin were analyzed on a Quanta 3D FEG scanning electron microscope (Thermo Fisher). The samples were immobilized onto an adhesive carbon conduction tab (Plano Carbon, Plano GmbH) and sputtered with platinum. The acceleration voltage of the electron microscope was 3 kV, and pictures were taken with a magnification of 100–25 000.

Atomic Force Microcopy: A total of 3 cTE samples prepared at 50 °C and isolated mature elastin from bovine ligamentum nuchae were analyzed by atomic force microscopy (AFM) using a JPK NanoWizard IV BioAFM (Bruker, Berlin, Germany) instrument mounted to an optical inverted microscope.

To determine topographical as well as mechanical properties, fast nanoindentation (Quantitative Imaging Mode) in a buffer solution (PBS) was applied. Here, the AFM investigations were carried out to measure a section of 2 × 2 µm^2 and 5 × 5 µm^2 with a resolution of 256 × 256 pixel^2 to represent the morphological nature of the layers as well as elastic modulus. The force constant calibration of used standard silicon qp-BioT (nanosensors) cantilevers was performed by using the thermal noise method.[50] In the post-processing procedure, the elastic modulus E was calculated from the indentation curves using an advanced Hertzian model.[51]

Coupling of PQQ to Magnetic Beads: Dynabeads M-270 Amine was obtained as an aqueous suspension at $\approx$2 × 10^9 beads per mL ($\hat{=}$ 30 mg mL^{-1}). PQQ was prepared as a stock solution in 0.1 M MES buffer (pH 4.5) at a concentration of 4 mg mL^{-1}. EDC ∎ HCl and NHS were prepared as stock solutions in ddH_2O at concentrations of 12.35 and 15 mg mL^{-1}, respectively. Fresh EDC and NHS stock solutions were mixed in equal volumes prior to use. The beads were washed twice with one volume of 0.1 M MES buffer (pH 4.5). Thirty micrograms PQQ per 10^8 beads were preincubated for 15 min at room temperature with 100 µL EDC/NHS mixture per mg of ligand to form PQQ-NHS ester. PQQ-NHS ester was subsequently added to the beads and incubated in one volume for 2 h at room temperature at 800 rpm on a thermomixer (Eppendorf AG, Hamburg, Germany). The reaction was quenched by adding 10 mM NH_2OH followed by further incubation at room temperature for 15 min in the thermomixer at 800 rpm. The supernatant was removed and the remaining amino groups on the surface of the beads were saturated with NHS-activated acetic acid. Therefore, an aqueous blocking mixture was prepared containing a fivefold excess of acetic acid with respect to moles of PQQ. For this, acetic acid was preincubated with EDC ∎ HCl and NHS in a molar ratio of 1:2:1 prepared from 1 M acetic acid and the EDC ∎ HCl and NHS stock solutions. The preincubated mixture was subsequently added to one volume of PQQ-functionalized beads and incubated for 1 h at room temperature in a thermomixer at 800 rpm. The reaction was quenched by adding 10 mM NH_2OH. The supernatant was removed, and the beads were washed twice with storage buffer (50 mM phosphate buffer, pH 7.4) and stored in one volume of this buffer at 4 °C until usage.

Recycling Test of PQQ-Beads: The recycling capability of the PQQ-functionalized magnetic beads was tested with a small synthetic peptide resembling the lysine-rich cross-linking pattern of domain 19 of human TE. The peptide sequence was H_2N-AAKAAAKAAKYG-NH$_2$ (monoisotopic mass 1118.66 Da). Two hundred fifty microliters of a 20 mg mL^{-1} peptide solution in 50 mM phosphate buffer (pH 8) and 4 mM $CuSO_4$ was added to 4 × 10^8 PQQ-functionalized beads (calculated according to the initial bead concentration) and subsequently incubated at 40 °C and 800 rpm on a thermomixer for 24 h. The supernatant was removed, and the beads were washed and stored as previously described. This procedure was repeated with the same batch of PQQ-functionalized beads. The supernatant was desalted using C18-ZipTips (Merck Millipore) according to the manufacturer's protocol and subsequently subjected to matrix-assisted laser desorption/ionization time-of-flight (MALDI-TOF) MS (Voyager-DE Pro, Sciex, Darmstadt, Germany). For this, the sample solution was mixed in a 1:9 (v/v) ratio with a 10 mg mL^{-1} stock solution of α-cyano-4-hydroxycinnamic acid prepared in ddH_2O/ACN (1:1 (v/v)) containing 0.1% TFA. One microliter of matrix-sample-mixture was transferred to the sample plate and air-dried. Measurements were performed

operating in the positive ion linear mode at a total acceleration voltage of 25 kV, grid voltage set to 93%, 0.15% guide wire voltage, and an extraction delay of 550 ns. For each sample, spot data of 500 single shot measurements were accumulated to the final mass spectrum.

The third reaction cycle with the same batch of PQQ-functionalized beads was performed with recombinant TE as the target molecule. Therefore, 4×10^8 PQQ-functionalized beads (calculated according to the initial bead concentration) were separated from the storage buffer and added to 500 µL of a TE solution (10 mg mL^{-1}) in 50 mM phosphate buffer (pH 8). The reaction mixture was incubated for 24 h in a thermomixer at 350 rpm and 40 °C. Subsequently, the beads were removed from the sample, and proteolytic digestions using PE (enzyme-substrate ratio 1:50 (w/w)) and trypsin (enzyme-substrate ratio 1:100 (w/w)) were performed as described above. Samples were subsequently subjected to HPLC-MS and peptide sequencing as described.

Conflict of Interest

The authors declare no conflict of interest.

Author Contributions

T.H. performed data curation. T.H., W.H., J.B., H.S., M.Mend., and M.Menz. performed formal analysis. T.H., W.H., J.B., H.S., M.Menz., M.Mend., and C.E.H.S. performed the investigation. T.H. performed visualization. T.H., M.Mend., J.B, H.S., and C.E.H.S. performed methodology. T.H. performed writing the original draft. C.E.H.S., T.G., and M.P. performed writing review and editing. C.E.H.S. and M.P. performed funding acquisition. C.E.H.S. performed conceptualization and project administration.

Data Availability Statement

The data that support the findings of this study are available from the corresponding author upon reasonable request.

[1] C. E. H. Schmelzer, L. Duca, *FEBS J.* **2022**, *289*, 3704.
[2] R. B. Rucker, M. A. Dubick, *Environ. Health Perspect.* **1984**, *55*, 179.
[3] E. C. Davis, *Histochemistry* **1993**, *100*, 17.
[4] S. D. Shapiro, S. K. Endicott, M. A. Province, J. A. Pierce, E. J. Campbell, *J. Clin. Invest.* **1991**, *87*, 1828.
[5] B. Vrhovski, A. S. Weiss, *Eur. J. Biochem.* **1998**, *258*, 1.
[6] Z. Indik, H. Yeh, N. Ornstein-Goldstein, U. Kucich, W. Abrams, J. C. Rosenbloom, J. Rosenbloom, *Am J. Med. Genet.* **1989**, *34*, 81.
[7] A. Borel, D. Eichenberger, J. Farjanel, E. Kessler, C. Gleyzal, D. J. S. Hulmes, P. Sommer, B. Font, *J. Biol. Chem.* **2001**, *276*, 48944.
[8] S. R. Pinnell, G. R. Martin, *Proc. Natl. Acad. Sci. USA* **1968**, *61*, 708.
[9] R. C. Siegel, S. R. Pinnell, G. R. Martin, *Biochemistry* **1970**, *9*, 4486.
[10] C. E. H. Schmelzer, A. Heinz, H. Troilo, M. P. Lockhart-Cairns, T. A. Jowitt, M. F. Marchand, L. Bidault, M. Bignon, T. Hedtke, A. Barret, J. C. Mcconnell, M. J. Sherratt, S. Germain, D. J. S. Hulmes, C. Baldock, L. Muller, *FASEB J.* **2019**, *33*, 5468.
[11] C. U. Schräder, A. Heinz, P. Majovsky, B. Karaman Mayack, J. Brinckmann, W. Sippl, C. E. H. Schmelzer, *J. Biol. Chem.* **2018**, *293*, 15107.
[12] T. Hedtke, C. U. Schräder, A. Heinz, W. Hoehenwarter, J. Brinckmann, T. Groth, C. E. H. Schmelzer, *FEBS J.* **2019**, *286*, 3594.
[13] C. E. H. Schmelzer, T. Hedtke, A. Heinz, *IUBMB Life* **2020**, *72*, 842.
[14] L. I. Smith-Mungo, H. M. Kagan, *Matrix Biol.* **1998**, *16*, 387.
[15] M. Akagawa, K. Suyama, *Biochem. Biophys. Res. Commun.* **2001**, *281*, 193.
[16] A. C. Mora Huertas, C. E. H. Schmelzer, W. Hoehenwarter, F. Heyroth, A. Heinz, *Biochimie* **2016**, *128-129*, 163.
[17] M. J. Sherratt, *Age (Dordr)* **2009**, *31*, 305.
[18] G. C. Yeo, B. Aghaei-Ghareh-Bolagh, E. P. Brackenreg, M. A. Hiob, P. Lee, A. S. Weiss, *Adv. Healthcare Mater.* **2015**, *4*, 2530.
[19] C. Anthony, *Antioxid. Redox Signal* **2001**, *3*, 757.
[20] T. Kumazawa, H. Seno, T. Urakami, T. Matsumoto, O. Suzuki, *Biochim. Biophys. Acta* **1992**, *1156*, 62.
[21] A. Lang, J. P. Klinman, *eLS* **2013**.
[22] C. Anthony, *Biochem. J.* **1996**, *320*, 697.
[23] P. R. Williamson, H. M. Kagan, *J. Biol. Chem.* **1987**, *262*, 8196.
[24] C. M. Bellingham, M. A. Lillie, J. M. Gosline, G. M. Wright, B. C. Starcher, A. J. Bailey, K. A. Woodhouse, F. W. Keeley, *Biopolymers* **2003**, *70*, 445.
[25] A. Heinz, C. U. Schräder, S. Baud, F. W. Keeley, S. M. Mithieux, A. S. Weiss, R. H. H. Neubert, C. E. H. Schmelzer, *Matrix Biol.* **2014**, *38*, 12.
[26] G. Francis, R. John, J. Thomas, *Biochem. J.* **1973**, *136*, 45.
[27] A. W. Clarke, E. C. Arnspang, S. M. Mithieux, E. Korkmaz, F. Braet, A. S. Weiss, *Biochemistry* **2006**, *45*, 9989.
[28] Y. Tu, S. G. Wise, A. S. Weiss, *Micron* **2010**, *41*, 268.
[29] I. Gonzalez De Torre, M. Alonso, J.-C. Rodriguez-Cabello, *Front. Bioeng. Biotechnol.* **2020**, *8*, 657.
[30] L. Mbundi, M. González-Pérez, F. González-Pérez, D. Juanes-Gusano, J. C. Rodríguez-Cabello, *Front. Mater.* **2021**, *7*, 601795.
[31] A. K. Varanko, J. C. Su, A. Chilkoti, *Ann. Rev. Biomed. Eng.* **2020**, *22*, 343.
[32] B. B. Aaron, J. M. Gosline, *Biopolym.: Orig. Res. Biomol.* **1981**, *20*, 1247.
[33] P. Geneste, M. L. Bender, *Proc. Natl. Acad. Sci. USA* **1969**, *64*, 683.
[34] J. C. Powers, B. F. Gupton, A. D. Harley, N. Nishino, R. J. Whitley, *Biochim. Biophys. Acta* **1977**, *485*, 156.
[35] M. A. Shah, P. R. Bergethon, A. M. Boak, P. M. Gallop, H. M. Kagan, *Biochim. Biophys. Acta* **1992**, *1159*, 311.
[36] N. R. Davis, R. A. Anwar, *J. Am. Chem. Soc.* **1970**, *92*, 3778.
[37] B. Bochicchio, A. Laurita, A. Heinz, C. E. H. Schmelzer, A. Pepe, *Biomacromolecules* **2013**, *14*, 4278.
[38] M. Akagawa, K. Suyama, *Connect. Tissue Res.* **2000**, *41*, 131.
[39] C. Franzblau, B. Faris, R. Papaioannou, *Biochemistry* **1969**, *8*, 2833.
[40] R. W. Lent, B. Smith, L. L. Salcedo, B. Faris, C. Franzblau, *Biochemistry* **1969**, *8*, 2837.
[41] R. Lent, C. Franzblau, *Biochem. Biophys. Res. Commun.* **1967**, *26*, 43.

[42] S. M. Partridge, *Gerontologia* **1969**, *15*, 85.

[43] F. Nakamura, K. Suyama, *Anal. Biochem.* **1994**, *223*, 21.

[44] J. A. Zahn, D. J. Bergmann, J. M. Boyd, R. C. Kunz, A. A. Dispirito, *J. Bacteriol.* **2001**, *183*, 6832.

[45] E. Shinagawa, H. Toyama, K. Matsushita, P. Tuitemwong, G. Theeragool, O. Adachi, *Biosci. Biotechnol. Biochem.* **2006**, *70*, 850.

[46] N. Hobara, A. Watanab, M. Kobayashi, T. Tsuji, Y. Gomita, Y. Araki, *Pharmacology* **1988**, *37*, 264.

[47] D. K. Summers, D. J. Sherratt, *EMBO J.* **1988**, *7*, 851.

[48] M. Jenzsch, S. Gnoth, M. Kleinschmidt, R. Simutis, A. Lübbert, *Bioprocess Biosyst. Eng.* **2006**, *29*, 315.

[49] M. Götze, J. Pettelkau, S. Schaks, K. Bosse, C. H. Ihling, F. Krauth, R. Fritzsche, U. Kühn, A. Sinz, *J. Am. Soc. Mass Spectrom.* **2012**, *23*, 76.

[50] J. E. Sader, J. W. M. Chon, P. Mulvaney, *Rev. Sci. Instrum.* **1999**, *70*, 3967.

[51] A. Renger, *Angew. Math. Mech.* **1989**, *69*, 214.